Published in final edited form as:
J Biomech. 2011 June 3; 44(9): 1817–1820. doi:10.1016/j.jbiomech.2011.04.009.

Anatomic variation in the elastic inhomogeneity and anisotropy of human femoral cortical bone tissue is consistent across multiple donors

David J. Rudy, **Justin M. Deuerling**, **Alejandro A. Espinoza Orías**[1], and **Ryan K. Roeder**
Department of Aerospace and Mechanical Engineering University of Notre Dame Notre Dame, IN 46556

Abstract

Numerical models commonly account for elastic inhomogeneity in cortical bone using power-law scaling relationships with various measures of tissue density, but limited experimental data exists for anatomic variation in elastic anisotropy. A recent study revealed anatomic variation in the magnitude and anisotropy of elastic constants along the entire femoral diaphysis of a single human femur (Espinoza Orías *et al*., 2009). The objective of this study was to confirm these trends across multiple donors while also considering possible confounding effects of the anatomic quadrant, apparent tissue density, donor age, and gender. Cortical bone specimens were sampled from the whole femora of nine human donors at 20, 50, and 80% of the total femur length. Elastic constants from the main diagonal of the reduced fourth-order tensor were measured on hydrated specimens using ultrasonic wave propagation. The tissue exhibited orthotropy overall and at each location along the length of the diaphysis ($p<0.0001$). Elastic anisotropy increased from the mid-diaphysis toward the epiphyses ($p<0.05$). The increased elastic anisotropy was primarily caused by a decreased radial elastic constant (C_{11}) from the mid-diaphysis toward the epiphyses ($p<0.05$), since differences in the circumferential (C_{22}) and longitudinal (C_{33}) elastic constants were not statistically significant ($p>0.29$). Anatomic variation in intracortical porosity may account for these trends, but requires further investigation. The apparent tissue density was positively correlated with the magnitude of each elastic constant ($p<0.0001$, $R^2>0.46$), as expected, but was only weakly correlated with C_{33}/C_{11} ($p<0.05$, $R^2=0.04$) and not significantly correlated with C_{33}/C_{22} and C_{11}/C_{22}.

Keywords

Anisotropy; Cortical Bone; Elastic Constants; Femur; Ultrasound

Correspondence: Ryan K. Roeder, Ph.D. Associate Professor Department of Aerospace and Mechanical Engineering Bioengineering Graduate Program 148 Multidisciplinary Research Building University of Notre Dame Notre Dame, IN 46556 Phone: (574) 631-7003 Fax: (574) 631-2144 rroeder@nd.edu.
[1]Current Address: Department of Orthopaedic Surgery Rush University Medical Center Chicago, IL 60612

Conflict of interest statement None declared.

1. INTRODUCTION

Elastic inhomogeneity in human cortical bone tissue is commonly accounted for by power-law scaling relationships with apparent tissue density, mineral density, or porosity (Hernandez *et al.*, 2001; Keller *et al.*, 1990; Shaffler and Burr, 1988; Zioupos *et al.*, 2008), but limited experimental data exists for anatomic variation in elastic anisotropy (Espinoza Orías *et al*., 2009). Experimental investigations of elastic anisotropy and inhomogeneity in cortical bone tissue have typically, for expediency, used specimens excised from the femoral mid-diaphysis. However, the proximal and distal ends of the diaphysis are more clinically relevant to common orthopaedic procedures and adaptive responses to mechanical loading.

Ultrasonic wave propagation has been used to enable non-destructive measurement of elastic constants on small specimens which can be sampled from various anatomic locations (Ashman *et al.*, 1984; Van Buskirk *et al.*, 1981). A recent study showed that elastic constant magnitudes decreased and elastic anisotropy increased from the mid-diaphysis toward the epiphyses of a human femur (Espinoza Orías *et al.*, 2009). The elastic symmetry of tissue in the distal and extreme proximal portions of the diaphysis was orthotropic, but was reasonably approximated as transversely isotropic near the mid-diaphysis. These trends were significantly correlated with the apparent tissue density and were suggested to be useful for numerical models of the human femur accounting for anisotropic and inhomogeneous tissue properties. However, a limitation was that tissue was sampled from a single elderly male donor. Therefore, the objective of this study was to confirm the above anatomic trends across multiple donors while also considering possible confounding effects of the anatomic quadrant, tissue density, donor age, and gender.

2. MATERIALS AND METHODS

Whole femora were harvested from the lower extremity of nine human donors, including six females (ages 41, 59, 73, 89, 93, and 99) and three males (ages 18, 53, and 78), presenting no toxicology or bone-related pathology. All tissues were obtained post-mortem with prior donor consent following protocol approved by the Notre Dame Human Subjects Institutional Review Board. Each femur was stored in a freezer at −20°C wrapped with gauze soaked in phosphate-buffered saline. A total of 108 parallelepiped cortical bone specimens (12 specimens/donor) were prepared from each anatomic quadrant at 20, 50, and 80% of the total femur length (Fig. 1a), which corresponded to locations previously shown to exhibit significant differences in elastic anisotropy for a single donor (Espinoza Orías *et al*., 2009). An orthogonal curvilinear coordinate system with radial (1), circumferential (2), and longitudinal (3) axes was defined by the anatomic shape of the femoral diaphysis (Fig. 1b).

Longitudinal elastic constants from the main diagonal of the reduced fourth-order stiffness tensor were measured on hydrated specimens using the pulse-transmission method for ultrasonic wave propagation as,

$$C_{ii}=\rho \cdot v_{ii}^2 \,(i=1,2,3) \tag{1}$$

where ρ is the apparent tissue density and v_{ii} is the longitudinal wave velocity in the *i*-th specimen direction. The apparent tissue density was measured using Archimedes' principle as,

$$\rho=\frac{M}{M-S}\cdot\rho_w \tag{2}$$

where M is the specimen mass while saturated with de-ionized (DI) water, S is the apparent specimen mass while submerged in DI water, and ρ_w is the density of DI water (ASTM, 1999). The ultrasonic wave velocity was measured using 2.25 MHz transducers (Models 5800, V106RM and V154RM, Panametrics, Inc., Waltham, MA) as $v_{ii} = d_i/\Delta t$, where d_i is the specimen dimension measured using digital calipers (±0.01 mm accuracy) and Δt is the time delay for wave transmission measured using an oscilloscope (±10 ns accuracy). The system accuracy was verified on a 5 mm steel gauge block before and after measurements on bone specimens. The coefficient of variation (precision) for thirty repeated measurements was previously measured as 1.3% (Espinoza Orías *et al.*, 2009). Elastic anisotropy was characterized by the ratio of orthogonal elastic constants (Hasegawa *et al.*, 1994; Takano *et al.*, 1996). Shear elastic constants (C_{44}, C_{55}, and C_{66}) were also measured for a subset of the donors and are reported in Appendix A as Supplementary Material. A detailed description of the methods for ultrasonic wave propagation is available elsewhere (Espinoza Orías *et al.*, 2009).

The nominal specimen size was approximately 5×5×5 mm, although the radial dimension was maximized within the available cortical thickness. Six specimens were removed from the analysis due to exhibiting a small radial thickness (<1.5 mm) that inhibited accurate measurement of the longitudinal and circumferential elastic constants by compromising the bulk wave assumption (Schwartz-Dabney and Dechow, 2002) and specimen-transducer contact. The overall mean (±standard deviation) radial specimen thickness was 3.3 (±1.4) mm. A pilot study was conducted with bovine cortical bone to confirm that the accuracy of measured ultrasonic wave velocities was independent of the radial specimen thickness.

One-way analysis of variance (ANOVA) was used to examine the effect of the anatomic location (% total femur length) on elastic constant magnitude and anisotropy (JMP 8, SAS Institute Inc., Cary, NC). *Post hoc* comparisons were performed using the Tukey-Kramer HSD test. Multivariate analysis of covariance (ANCOVA) was used to examine possible confounding effects of the anatomic quadrant, apparent tissue density, donor age, and gender. Linear least squares regression was used to correlate elastic constant magnitudes and anisotropy with the apparent tissue density. The level of significance for all tests was 0.05.

3. RESULTS

Each elastic constant and anisotropy ratio exhibited statistically significant differences overall and at each given location along the length of the femoral diaphysis ($p<0.0001$, Tukey) with $C_{33}>C_{22}>C_{11}$ (Fig. 2). Therefore, the tissue exhibited orthotropy overall and at each location along the length of the diaphysis. The magnitude of C_{11} decreased from the mid-diaphysis toward the distal ($p<0.0001$, Tukey) and proximal ($p<0.05$) epiphyses, while C_{22} and C_{33} did not exhibit statistically significant differences ($p>0.29$) (Fig. 2a). The elastic anisotropy ratio C_{33}/C_{11} increased ($p<0.0001$, Tukey), C_{33}/C_{22} decreased ($p<0.05$), and C_{11}/C_{22} decreased ($p<0.0001$) toward the distal epiphysis; C_{33}/C_{11} increased ($p<0.05$, Tukey), C_{33}/C_{22} did not exhibit a statistically significant difference ($p=0.83$), and C_{11}/C_{22} decreased ($p<0.01$) toward the proximal epiphysis (Fig. 2b).

Multivariate analysis of covariance indicated a statistically significant effect of the anatomic location along the femoral diaphysis on the elastic constant magnitude and anisotropy ($p<0.0001$ for C_{11}, C_{22}, C_{33}/C_{11}, and C_{11}/C_{22}; $p<0.05$ for C_{33} and C_{33}/C_{22}), and that this effect was not confounded by the effects of anatomic quadrant, donor age, and gender which were all not statistically significant. The apparent tissue density exhibited a statistically significant effect on elastic constant magnitudes ($p<0.0001$) but not the anisotropy. In one-way ANOVA, the apparent tissue density was positively correlated with the magnitude of

each elastic constant ($p<0.0001$, $R^2>0.46$), as expected, but was only weakly correlated with C_{33}/C_{11} ($p<0.05$, $R^2=0.04$) and not significantly correlated with C_{33}/C_{22} and C_{11}/C_{22}.

The apparent tissue density decreased toward the distal epiphysis ($p<0.05$, Tukey), but did not exhibit a statistically significant difference toward the proximal epiphysis ($p=0.27$). Multivariate analysis of covariance indicated a statistically significant effect of the anatomic location along the femoral diaphysis ($p<0.10$), anatomic quadrant ($p<0.05$), and donor age ($p<0.005$) on the apparent tissue density.

The entire dataset, including data and analysis for shear elastic constants (C_{44}, C_{55}, and C_{66}), is available in Appendix A as Supplementary Material. Shear elastic constants and anisotropy ratios exhibited similar trends and correlations as those reported above for longitudinal elastic constants.

4. DISCUSSION

The results of this study confirmed trends previously reported for a single donor (Espinoza Orías *et al*., 2009) on multiple donors, although tissue specimens pooled from multiple donors exhibited orthotropy at all locations along the femoral diaphysis rather than transverse isotropy at the mid-diaphysis (Fig. 2). Elastic anisotropy increased from the mid-diaphysis toward the epiphyses (Fig. 2b). This trend was relatively robust and not influenced by anatomic quadrant, donor age, or gender. The increased elastic anisotropy was primarily caused by a decreased radial elastic constant (C_{11}) from the mid-diaphysis toward the epiphyses, since C_{22} and C_{33} did not change (Fig. 2a). In other words, decreases in C_{11} increased C_{33}/C_{11} and decreased C_{11}/C_{22} (Fig. 2b). Therefore, the observed anatomic variation in elastic anisotropy was primarily due to structural differences in the radial direction.

Variations in intracortical porosity along the length of the femoral diaphysis were previously hypothesized to account for differences in the radial elastic constant (Espinoza Orías *et al*., 2009). Variations may include changes in the size and shape of Haversian canals and resorption cavities, or an increase in the number and size of radially oriented Volkmann's canals and canaliculi. A previous study reported decreased E_3/E_2 (Young's moduli) with increased tissue porosity ($p<0.01$, $R^2=0.35$) (Dong and Guo, 2004). However, in the present study, the apparent tissue density was weakly correlated with C_{33}/C_{11} ($p<0.05$, $R^2=0.04$) and not significantly correlated with C_{33}/C_{22} and C_{11}/C_{22}. Moreover, the multivariate analysis suggested that the anatomic location along the femoral diaphysis and apparent tissue density were together able to account for 56–64% of the variability in elastic constants, but only 7–33% of the variability in elastic anisotropy.

A true scalar quantity like apparent tissue density or porosity would not be expected to influence a directional property like the anisotropy ratio. However, the spatial size, morphology, orientation, and distribution of pores along the length of the femur may contribute to the observed property variation independent of the porosity volume fraction. Finite element models on micro-computed tomography reconstructions with segmented intracortical porosity (Burghardt *et al*., 2010) could be utilized to investigate these effects on the elastic anisotropy.

Other structural features within the extracellular matrix may also be responsible for variations in elastic anisotropy. The apatite crystal orientation distribution was recently shown to exhibit the greatest influence on elastic anisotropy in a specimen-specific micromechanical model accounting for seven structural parameters across multiple length scales in human cortical bone (Deuerling *et al*., 2009). Apatite crystals in cortical bone are preferentially oriented along the longitudinal bone axis (Sasaki *et al*., 1989), but changes in

the orientation distribution also affect the elastic anisotropy (Deuerling *et al*., 2009). A micromechanical model accounting for effects of the apatite crystal orientation distribution could be combined with a finite element model accounting for the effects of intracortical porosity, in order to investigate and decouple these effects on the elastic anisotropy of cortical bone.

The data gathered in this study may be useful for numerical models of the femur in order to account for anatomic variations in elastic inhomogeneity *and* anisotropy in cortical bone (Bagge, 2000; Chavalier *et al*., 2009; Doblaré and Garcia, 2001; Jacobs *et al*., 1997; Lenaerts and van Lenthe, 2009; Taylor *et al*., 2002; Wirtz *et al*., 2001, 2003). However, a possible limitation of this study was that the determination of engineering coefficients requires assumptions regarding off-diagonal elastic constants due to the measurement of an incomplete stiffness tensor.

The statistical power in this study was sufficient to meet the study objective, but was not sufficient to examine differences in the magnitude and anisotropy of elastic constants with respect to the anatomic quadrant, donor gender, and donor age. Statistical power for the effect of location along the femoral diaphysis was greater than 0.99 for C_{11}, C_{22}, C_{33}/C_{11}, and C_{11}/C_{22}, and greater than 0.60 for C_{33} and C_{33}/C_{22}. Statistical power for the effects of the location along the femoral diaphysis, anatomic quadrant, and donor age on the apparent tissue density was 0.51, 0.65, and 0.85, respectively. Statistical power for the effect of the apparent tissue density on elastic constants was 1.00. All other effects exhibited statistical power less than 0.34 in the multivariate analysis.

Supplementary Material

Refer to Web version on PubMed Central for supplementary material.

Acknowledgments

This research was partially supported by the U.S. Army Medical Research and Material Command (W81XWH-06-1-0196) through the Peer-Reviewed Medical Research Program (PR054672) and the National Institutes of Health (AR052008).

REFERENCES

Ashman RB, Cowin SC, Van Buskirk WC, Rice JC. A continuous wave technique for the measurement of the elastic properties of cortical bone. Journal of Biomechanics. 1984; 17:349–361. [PubMed: 6736070]

ASTM Standard C373-88. Standard Test Method for Water Absorption, Bulk Density, Apparent Density and the Apparent Specific Gravity of Fired Whiteware Products. American Society for Testing Materials; West Conshohocken, PA: 1999.

Bagge M. A model of bone adaptation as an optimization process. Journal of Biomechanics. 2000; 33:1349–1357. [PubMed: 10940393]

Burghardt A, Kazakia G, Ramachandran S, Link T, Majumdar S. Age- and gender-related differences in the geometric properties and biomechanical significance of intracortical porosity in the distal radius and tibia. Journal of Bone and Mineral Research. 2010; 25:983–993. [PubMed: 19888900]

Chavalier Y, Pahr D, Zysset PK. The role of cortical shell and trabecular fabric in finite element analysis of the human vertebral body. Journal of Biomechanical Engineering. 2009; 131:111003. [PubMed: 20353254]

Deuerling JM, Yue W, Espinoza Orías AA, Roeder RK. Specimen-specific multiscale model for the anisotropic elastic constants of human cortical bone. Journal of Biomechanics. 2009; 42:2061–2067. [PubMed: 19664772]

Doblaré M, Garcia JM. Application of an anisotropic bone-remodelling model based on a damage-repair theory to the analysis of the proximal femur before and after total hip replacement. Journal of Biomechanics. 2001; 34:1157–1170. [PubMed: 11506786]

Dong XN, Guo XE. The dependence of transversely isotropic elasticity of human femoral cortical bone on porosity. Journal of Biomechanics. 2004; 37:1281–1287. [PubMed: 15212934]

Espinoza Orías AA, Renaud JE, Deuerling JM, Roeder RK. Anatomic variation in the elastic anisotropy of cortical bone tissue in the human femur. Journal of the Mechanical Behavior of Biomedical Materials. 2009; 2:255–263. [PubMed: 19627830]

Hasegawa K, Turner CH, Burr DB. Contribution of collagen and mineral to the elastic anisotropy of bone. Calcified Tissue International. 1994; 55:381–386. [PubMed: 7866920]

Hernandez CJ, Beaupré GS, Keller TS, Carter DR. The influence of bone volume fraction and ash fraction on bone strength and modulus. Bone. 2001; 29:74–78. [PubMed: 11472894]

Jacobs CR, Simo JC, Beaupré GS, Carter DR. Adaptive bone remodeling incorporating simultaneous density and anisotropy considerations. Journal of Biomechanics. 1997; 30:603–613. [PubMed: 9165394]

Keller TS, Mao Z, Spengler DM. Young's modulus, bending strength, and tissue physical properties of human compact bone. Journal of Orthopaedic Research. 1990; 8:592–603. [PubMed: 2355299]

Lenaerts L, van Lenthe GH. Multi-level patient-specific modeling of the proximal femur. A promising tool to quantify the effect of osteoporosis treatment. Philosophical Transactions of the Royal Society A. 2009; 367:2079–2093.

Sasaki N, Matsushima N, Ikawa N, Yamamura H, Fukuda A. Orientation of bone mineral and its role in the anisotropic mechanical properties of bone-transverse anisotropy. Journal of Biomechanics. 1989; 22:157–164. [PubMed: 2540205]

Schaffler M, Burr D. Stiffness of compact bone: effects of porosity and density. Journal of Biomechanics. 1988; 21:13–16. [PubMed: 3339022]

Schwartz-Dabney CL, Dechow PC. Accuracy of elastic property measurement in mandibular cortical bone is improved by using cylindrical specimens. Journal of Biomechanical Engineering. 2002; 124:714–723. [PubMed: 12596640]

Takano Y, Turner CH, Burr DB. Mineral anisotropy in mineralized tissues is similar among species and mineral growth occurs independently of collagen orientation in rats: Results from acoustic velocity measurements. Journal of Bone and Mineral Research. 1996; 11:1292–1301. [PubMed: 8864904]

Taylor WR, Roland E, Ploeg H, Hertig D, Klabunde R, Warner MD, Hobatho MC, Rakotomana L, Clift SE. Determination of orthotropic bone elastic constants using FEA and modal analysis. Journal of Biomechanics. 2002; 35:767–773. [PubMed: 12020996]

Van Buskirk WC, Cowin SC, Ward RN. Ultrasonic measurement of orthotropic elastic constants of bovine femoral bone. Journal of Biomechanical Engineering. 1981; 103:67–72. [PubMed: 7278184]

Wirtz DC, Schiffers N, Pandorf T, Radermacher K, Weichert D, Forst R. Critical evaluation of known bone materials properties to realize anisotropic FE-simulation of the proximal femur. Journal of Biomechanics. 2000; 33:1325–1330. [PubMed: 10899344]

Wirtz DC, Pandorf T, Porttheine F, Radermacher K, Schiffers N, Prescher A, Weichert D, Niethhard FU. Concept and development of an orthotropic FE model of the proximal femur. Journal of Biomechanics. 2003; 36:289–293. [PubMed: 12547369]

Zioupos P, Cook R, Hutchinson J. Some basic relationships between density values in cancellous and cortical bone. Journal of Biomechanics. 2008; 41:1961–1968. [PubMed: 18501911]

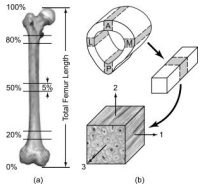

Figure 1.
Cortical bone specimens were sectioned from the diaphysis of whole human femora at (a) 20, 50, and 80% of the total femur length and (b) from each anatomic quadrant (A = anterior, M = medial, P = posterior, L = lateral), using an orthogonal curvilinear coordinate system (1 = radial, 2 = circumferential, 3 = longitudinal).

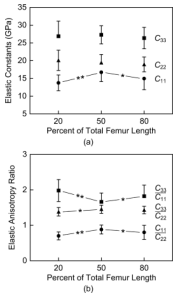

Figure 2.

Mean (a) elastic constants and (b) anisotropy ratios in the three orthogonal specimen axes measured along the length of the femoral diaphysis. Error bars show one standard deviation. Statistically significant differences existed between each elastic constant and anisotropy ratio at a given location along the length of the femoral diaphysis ($p < 0.0001$, Tukey). Asterisks denote statistically significant differences between elastic constants or anisotropy ratios at the mid-diaphysis compared to locations at the distal and proximal ends of the diaphysis (* $p < 0.05$, ** $p < 0.0001$, Tukey).